



## RESEARCH ARTICLE

# Novel *TG-FGFR1* and *TRIM33-NTRK1* transcript fusions in papillary thyroid carcinoma

Aleksandra Pfeifer<sup>1#</sup>  | Dagmara Rusinek<sup>1#</sup> | Jadwiga Żebracka-Gala<sup>1</sup> |  
 Agnieszka Czarniecka<sup>2</sup> | Ewa Chmielik<sup>3</sup> | Ewa Zembala-Nożyńska<sup>3</sup> | Bartosz Wojtaś<sup>4</sup> |  
 Bartłomiej Gielniewski<sup>4</sup> | Sylwia Szpak-Ulczoł<sup>1</sup> | Małgorzata Oczko-Wojciechowska<sup>1</sup> |  
 Jolanta Krajewska<sup>1</sup> | Joanna Polańska<sup>5</sup>  | Barbara Jarzab<sup>1</sup>

<sup>1</sup>Department of Nuclear Medicine and Endocrine Oncology, Maria Skłodowska-Curie Institute – Oncology Center Gliwice Branch, Gliwice, Poland

<sup>2</sup>Department of Oncological and Reconstructive Surgery, Maria Skłodowska-Curie Institute – Oncology Center Gliwice Branch, Gliwice, Poland

<sup>3</sup>Tumor Pathology Department, Maria Skłodowska-Curie Institute – Oncology Center Gliwice Branch, Gliwice, Poland

<sup>4</sup>Laboratory of Molecular Neurobiology, Neurobiology Center, Nencki Institute of Experimental Biology, Warsaw, Poland

<sup>5</sup>Faculty of Automatic Control, Electronics and Computer Science, Silesian University of Technology, Gliwice, Poland

## Correspondence

Aleksandra Pfeifer, Department of Nuclear Medicine and Endocrine Oncology, Maria Skłodowska-Curie Institute – Oncology Center, Wybrzeże Armii Krajowej 15, 44-101 Gliwice, Poland.

Email: aleksandra.pfeifer@io.gliwice.pl

## Funding information

POIG.02.01.00-00-166/08. Śląska BIO-FARMA. Centrum Biotechnologii, Bioinżynierii i Bioinformatyki; Polish National Center of Research and Development, Grant/Award Number: STRATEGMED2/267398/4/NCBR/2015; PL-Grid Infrastructure; Polish National Science Center, Grant/Award Number: DEC-2011/03/N/NZ2/03495

Papillary thyroid carcinoma (PTC) is most common among all thyroid cancers. Multiple genomic alterations occur in PTC, and gene rearrangements are one of them. Here we screened 14 tumors for novel fusion transcripts by RNA-Seq. Two samples harboring *RET/PTC1* and *RET/PTC3* rearrangements were positive controls whereas the remaining ones were negative regarding the common PTC alterations. We used Sanger sequencing to validate potential fusions. We detected 2 novel potentially oncogenic transcript fusions: *TG-FGFR1* and *TRIM33-NTRK1*. We detected 4 novel fusion transcripts of unknown significance accompanying the *TRIM33-NTRK1* fusion: *ZSWIM5-TP53BP2*, *TAF4B-WDR1*, *ABI2-MTA3*, and *ARID1B-PSMA1*. Apart from confirming the presence of *RET/PTC1* and *RET/PTC3* in positive control samples, we also detected known oncogenic fusion transcripts in remaining samples: *TFG-NTRK1*, *ETV6-NTRK3*, *MKRN1-BRAF*, *EML4-ALK*, and novel isoform of *CCDC6-RET*.

## KEYWORDS

papillary thyroid carcinoma, rearrangement, RNA-Seq, transcript fusion

## 1 | INTRODUCTION

Papillary thyroid carcinoma (PTC) is most common among all thyroid cancers. The most common driver alterations in PTC are point mutations in *BRAF* and *RAS* genes (*KRAS*, *HRAS*, and *NRAS*) and rearrangements of the *RET* gene (*RET/PTC* rearrangements). According to The Cancer Genome Atlas (TCGA) study, these alterations occur in 59.7%, 13%, and 6.3% of the PTC cases, respectively, and the total prevalence of gene rearrangements is 15%.<sup>1</sup>

Multiple gene rearrangements occur in PTC, and *RET/PTC* are the most prevalent ones.<sup>1</sup> *RET/PTC* rearrangements are associated with younger age and radiation exposure.<sup>2</sup> As documented in the previous studies, detection of these alterations in cytological specimens may be helpful in improving the accuracy of the diagnosis of PTC.<sup>3</sup> Multiple gene rearrangements can be screened using the molecular test Thyro-Seq; these rearrangements entail a high risk of cancer.<sup>4</sup> However, it is worth noting that gene rearrangements can also be found in some benign thyroid diseases.<sup>5</sup>

In recent years, our knowledge about genomic rearrangements and transcript fusions in PTC has widely expanded, mostly thanks to

# These authors contributed equally to this work.

RNA-Seq, what led to the detection of numerous novel gene rearrangements in PTC.<sup>1,6–11</sup> The most important was the detection of *ETV6-NTRK3*, which occurs in 2%–14.5% of PTC patients.<sup>8</sup> In PTCs, the most common 5' partner in gene rearrangements are *RET*, *BRAF*, *NTRK3*, *THADA*, *PPARG*, *NTRK1*, and *ALK*.<sup>1</sup> All of them, except *THADA*, code for proteins with tyrosine kinase domains.

Our study aimed to detect novel transcript fusions in PTC to expand the knowledge about genetic alterations in this malignancy.

## 2 | MATERIALS AND METHODS

### 2.1 | Samples

Fresh-frozen material from 14 PTCs was used in this study. Surgical procedures were performed in Maria Skłodowska-Curie Institute—Oncology Center, Gliwice Branch. The study was approved by the Bioethics Committee of Maria Skłodowska-Curie Institute—Oncology Center, Gliwice Branch. Informed consent was obtained from all patients.

The samples were selected from a group, in which common PTC mutations have been already analyzed: point mutations—*BRAF*<sup>V600E</sup> and mutations in codons 12, 13, and 61 of *HRAS*, *NRAS*, and *KRAS* genes with Sanger sequencing and rearrangements—*PAX8-PPARG*, *RET/PTC1*, and *RET/PTC3* with quantitative real-time polymerase chain reaction (qRT-PCR). Among 14 samples selected for RNA-Seq experiment, there was 1 sample positive for *RET/PTC1* rearrangement and 1 sample positive for *RET/PTC3* rearrangement. The remaining 12 samples were negative for *BRAF*<sup>V600E</sup> mutation, *HRAS*, *NRAS*, *KRAS* hotspot mutations, *PAX8-PPARG*, *RET/PTC1* and *RET/PTC3* rearrangements, with the exception of a few cases in which not all mutations were evaluated due to sample availability limitations (details in Supporting Information Table S1).

There were 3 males and 11 females in our study group diagnosed with classical (10 cases) and follicular (4 cases) PTC variants. Young patients were preferred during sample selection: the mean age at

diagnosis was 24 years, with a median of 26 years (range: 13–40 years). The mean and median tumor diameters were 17 mm and 15 mm, respectively (range 10–34 mm). Four PTCs were multifocal, 5 with capsule invasion, and 1 with vascular invasion. Lateral neck lymph node metastases were present in 7 patients. Neither local recurrence nor distant metastases were present in any patient from the study group. The histopathological characteristics of the tumors are given in Table 1.

### 2.2 | RNA-Seq

To detect novel fusion transcripts in PTC, we performed paired-end RNA-Seq on 12 PTC samples that were negative regarding most common PTC genetic alterations (*BRAF*<sup>V600E</sup> mutation, mutations in codons 12, 13, and 61 of *HRAS*, *NRAS*, and *KRAS* genes, *PAX8-PPARG*, *RET/PTC1*, and *RET/PTC3*). We also performed paired-end RNA-Seq experiment on 1 case with *RET/PTC1* and 1 case with *RET/PTC3* as positive controls.

Total RNA was extracted from homogenized frozen tissue using Mini Kits (Qiagen GmbH, Hilden, Germany). RNA quantity was measured by NanoDrop ND-1000 (Thermo Scientific, Wilmington, DE) minispectrophotometer whereas its quality was estimated by Agilent 2100 using RNA 6000 Nano Assay (Agilent Technologies, Santa Clara, CA). Only high-quality RNA (RNA Integrity Number > 6.5) was used. Sequencing libraries were prepared with the TruSeq RNA Sample Preparation Kit v2 SetA (Illumina Inc., San Diego, CA), following the manufacturer's protocol.

Oligo(dT) magnetic beads Agencourt Ampure XP (Beckman Coulter Inc. Brea, CA) were used to isolate poly(A) RNA from the total RNA samples. The mRNA was fragmented by heating at 94°C for 8 minutes. First-strand cDNA was synthesized using random hexamer primers for 10 minutes at 25°C, 50 minutes at 42°C, and 15 minutes at 70°C. After the synthesis of the first strand, dNTPs, DNA Polymerase I and RNaseH were added to synthesize second-strand cDNA for 1 hour at 16°C. The ends of double-stranded cDNA were repaired by using End Repair Mix. A single "A" nucleotide was added to the 3'

**TABLE 1** Histopathological characteristics of 14 PTC samples included in this study

Sample	Sex	Age (years)	Histology	Tumor diameter (mm)	Multifocality	Capsule invasion	Metastasis to lateral neck lymph nodes	Vascular invasion
NIS164	F	29	Classic	34	Multifocal	Yes	No	No
NIS203	M	13	Classic	32	Multifocal	Yes	Yes	Yes
NIS207	F	16	Classic	15	Multifocal	Yes	No	No
NIS280	F	19	Follicular	10	Unifocal	No	No	No
PTC006	M	32	Classic	14	Unifocal	No	No	No
PTC100	F	25	Follicular	15	Multifocal	Yes	Yes	No
PTC102	F	15	Classic	20	Unifocal	No	Yes	No
PTC106	F	17	Classic	11	Unifocal	No	No	No
PTC113	F	23	Classic	18	Unifocal	No	Yes	No
PTC131	F	29	Classic	15	Unifocal	No	Yes	No
PTC135	F	29	Follicular	14	Unifocal	No	Yes	No
PTC174	M	27	Classic	15	Unifocal	No	No	No
PTC18	F	40	Follicular	10	Unifocal	No	No	No
PTC181	F	29	Classic	16	Unifocal	Yes	Yes	No

ends of the cDNA molecules and the fragments were ligated to the paired-end adapters. The purified cDNA was amplified by 15 cycles of PCR for 10 seconds at 98°C, 30 seconds at 60°C, and 30 seconds at 72°C using PCR primers. The quality of the resulting sequencing libraries were determined on a High Sensitivity DNA Kit using an Agilent 2100 Bioanalyser (Agilent Technologies, Santa Clara, CA) and concentration of the libraries was determined on Qubit (Invitrogen, Carlsbad, CA). The mRNASeq libraries were sequenced on a HiSeq1500 device (Illumina Inc., San Diego, CA) to generate 2×120 or 2×106 bp paired-end reads.

## 2.3 | RNA-Seq data analysis

Read's quality was assessed using FastQC version 0.9.3.<sup>12</sup> Raw FASTQ data were trimmed and filtered using Prinseq-lite version 0.20.4, and only high-quality reads were used in the further analysis.<sup>13</sup>

Fusion transcripts detection was performed using three bioinformatics tools in order to achieve a high sensitivity: TopHat-Fusion (TopHat version 2.0.10),<sup>14</sup> ChimeraScan version 0.4.5,<sup>15</sup> and SnowShoes-FTD version 2.0 Build 37.<sup>16</sup> Fusion transcripts detected with these tools were further filtered with in-house tools in order to filter out false positive findings (details provided in supplementary methods). Genome version GRCh37/hg19 was used in all these analyses.

The list of fusion transcripts present in normal samples was obtained from the paper published by Babiceanu et al.<sup>17</sup>

## 2.4 | Validation of detected transcript fusions with Sanger sequencing

Validation of novel transcript fusions was performed with the use of Sanger's direct sequencing method on the 3130xl Genetic Analyzer (Life Technologies, Carlsbad, CA) with ABI PRISM 1.1 BigDye Terminator Cycle Sequencing Ready Reaction Kit (Life Technologies). Before sequencing, RNA (200 ng) was converted to cDNA with the Omniscript RT Kit (Qiagen GmbH). The reaction was carried out for 1 hour at 37°C in a volume of 20 µL using a mixture of 1× concentrated buffer (2 µL; Omniscript RT Kit), 5× concentrated dNTPs (2 µL; Omniscript RT Kit), 4 U/µl RT-O polymerase (1 µL; Omniscript RT Kit), 50 µM random nonamers (1.6 µL), and 1× concentrated RiboLock RNase inhibitor (1 µL; Fermentas Thermo Fisher Scientific, Waltham, MA). Obtained cDNA was used as a template in PCR reactions, in which each amplicon was amplified using specific primers designed with the Primer3 Input software available on the website <http://frodo.wi.mit.edu/> (for primer sequences and annealing temperatures used in PCR reactions, see Supporting Information Table S2). Each amplicon contained sequences of both rearranged genes. The PCR products were visualized by electrophoresis in a 2% agarose gel in the presence of bromide ethidium (0,3 µL/mL), cleaned with Exo I (volume 0.6 µL; concentration 10 U/µl; Life Technologies) and Sap (volume 0.6 µL; concentration 2 U/µl; Boehringer Mannheim GmbH, Germany; Life Technologies) enzymes mixture according to manufacturer's recommendations and then sequenced as described earlier.

## 3 | RESULTS

### 3.1 | Detection of fusion transcripts by RNA-Seq

In order to detect novel fusion transcripts in PTC, we performed paired-end RNA-Seq experiment on 14 PTC tumor samples. After filtering and trimming of raw reads, we obtained an average of 13.5 million read pairs in each sample. The read length was 120 bp in 6 samples and 50 bp in 8 samples (Supporting Information Table S3).

We detected 28 fusion events by TopHat-Fusion, 96 by ChimeraScan, and 34 by SnowShoes-FTD (Supporting Information Tables S4-S6). In total, we detected 126 fusion events. Seventy-three of them were read-throughs or were detected in normal samples as depicted by Babiceanu et al.<sup>17</sup> and these were beyond our interest (Supporting Information Table S7). The remaining 53 fusion transcripts, which were not read-throughs and not detected in normal samples, were further manually inspected (Supporting Information Table S8).

We manually selected candidate fusion transcripts potentially tumorigenic, which involved genes with known cancer-associated functions. We also selected all candidate fusion transcripts that were detected by more than one program. Final list consisted of 18 transcript fusions (Table 2), found in 11 of 14 tumor samples.

The following novel transcript fusions were detected with RNA-Seq method: *TG-FGFR1*, *FGFR1-TG*, two isoforms of *TRIM33-NTRK1*, *ARID1B-PSMA1*, *TAF4B-WDR1*, *ABI2-MTA3*, *ZSWIM5-TP53BP2*, and the novel isoform of *CCDC6-RET*. *RET/PTC1* and *RET/PTC3* fusion transcripts were found, as expected, in positive control samples. We also detected known oncogenic fusion transcripts: *TFG-NTRK1*, *ETV6-NTRK3* (in three samples), *MKRN1-BRAF*, and *EML4-ALK*.

### 3.2 | Validation of fusion transcripts

We performed validation by direct Sanger sequencing for all 9 novel fusion transcripts. We confirmed the existence of 8/9 fusions: *TG-FGFR1*, *FGFR1-TG*, one isoform of *TRIM33-NTRK1* (with a breakpoint in chr1:114952806-chr1:156845312), *ARID1B-PSMA1*, *TAF4B-WDR1*, *ABI2-MTA3*, *ZSWIM5-TP53BP2* as well as the novel isoform of *CCDC6-RET* (Figures 1 and 2; Supporting Information Figures S1-S6). We did not confirm the second *TRIM33-NTRK1* fusion isoform, with a breakpoint in chr1:114952806-chr1:156846192. When we used primers designed for that *TRIM33-NTRK1* isoform, we did not observe the expected sequence.

### 3.3 | Novel fusion transcripts

We detected 2 novel in-frame fusion transcripts, which are potential driver alterations: *TG-FGFR1* and *TRIM33-NTRK1*.

We identified a novel fusion of thyroglobulin (*TG*) and fibroblast growth factor receptor 1 (*FGFR1*) in sample NIS164 (Figure 1). The sample was a multifocal classic PTC tumor, 34 mm in diameter, with capsule invasion, no metastasis to lateral neck lymph nodes, and no vascular invasion. The patient was a 29-year-old female. *TG* and *FGFR1* genes are localized at 8q24 and 8p11. *TG-FGFR1* juxtaposes exons 1-47 of *TG* (ENST00000220616) to exons 9-18 of *FGFR1* (ENST00000447712). The fusion protein is predicted to include 1-2730 amino acids (AA) of *TG* and 361-822 AA of *FGFR1*. All domains encoded

**TABLE 2** List of candidate fusion transcripts detected in PTC with RNA-Seq method

Sample	5' Chromosome	3' Chromosome	5' Breakpoint	3' Breakpoint	5' Symbol	3' Symbol	5' Entrez	3' Entrez	Exon boundary Fusion <sup>a</sup>	Sanger validation results	Comment
1	NIS164 chr8	chr8	134 145 904	38 277 253	TG	FGFR1	7038	2260	Yes	Positive	Novel potentially oncogenic fusion transcript
2	NIS164 chr8	chr8	38 279 315	134 146 920	FGFR1	TG	2260	7038	Yes	Positive	Reciprocal of novel fusion transcript
3	NIS203 chr10	chr10	51 582 939	43 612 032	NCOA4	RET	8031	5979	Yes	-	Positive control (RET/PTC3)
4	NIS207 chr3	chr1	100 455 548	156 844 363	TFG	NTRK1	10 342	4914	Yes	-	Known oncogenic fusion transcript
5	NIS207 chr3	chr1	100 455 560	156 844 363	TFG	NTRK1	10 342	4914	Yes	-	Known oncogenic fusion transcript
6	PTC100 chr12	chr15	12 006 495	88 576 276	ETV6	NTRK3	2120	4916	Yes	-	Known oncogenic fusion transcript
7	PTC102 chr10	chr10	61 665 880	43 612 032	CCDC6	RET	8030	5979	Yes	-	Positive control (RET/PTC1)
8	PTC106 chr10	chr10	61 554 231	43 612 032	CCDC6	RET	8030	5979	Yes	Positive	Novel isoform of oncogenic fusion transcript
9	PTC113 chr7	chr7	140 158 807	140 481 493	MKRN1	BRAF	23 608	673	Yes	-	Known oncogenic fusion transcript
10	PTC131 chr1	chr1	114 952 806	156 845 312	TRIM33	NTRK1	51 592	4914	Yes	Positive	Novel potentially oncogenic fusion transcript
11	PTC131 chr1	chr1	114 952 806	156 846 192	TRIM33	NTRK1	51 592	4914	Yes	Negative	-
12	PTC131 chr1	chr1	45 671 428	223 972 016	ZSWIM5	TP53BP2	57 643	7159	Yes	Positive	Novel fusion transcript
13	PTC131 chr18	chr4	23 847 587	10 080 625	TAF4B	WDR1	6875	9948	Yes	Positive	Novel fusion transcript
14	PTC131 chr2	chr2	204 245 107	42 867 313	ABI2	MTA3	10 152	57 504	Yes	Positive	Novel fusion transcript
15	PTC131 chr6	chr11	157 150 555	14 540 587	ARID1B	PSMA1	57 492	5682	Yes	Positive	Novel fusion transcript
16	PTC135 chr12	chr15	12 006 495	88 576 276	ETV6	NTRK3	2120	4916	Yes	-	Known oncogenic fusion transcript
17	PTC174 chr2	chr2	42 522 656	29 446 394	EML4	ALK	27 436	238	Yes	-	Known oncogenic fusion transcript
18	PTC181 chr12	chr15	12 006 495	88 576 276	ETV6	NTRK3	2120	4916	Yes	-	Known oncogenic fusion transcript

<sup>a</sup> Exon boundary fusion is a fusion transcript in which both sides of the junction are known exon boundaries of the parental genes.

by TG and the whole protein kinase domain encoded by *FGFR1* are retained in this fusion. In NIS164 sample harboring *TG-FGFR1*, also a reciprocal fusion *FGFR1-TG* was detected, which fuses exons 1-8 of *FGFR1* to exon 48 of *TG* (Supporting Information Figure S1).

We identified a novel fusion of tripartite motif containing 33 (*TRIM33*) and neurotrophic receptor tyrosine kinase 1 (*NTRK1*) in PTC131 sample (Figure 2). The sample was a unifocal classic PTC tumor, 15 mm in diameter, with metastasis to lateral neck lymph nodes, no capsule invasion, and no vascular invasion. The patient was a 29-year-old female. The *TRIM33* and *NTRK1* genes are localized at 1p13 and 1q23. *TRIM33-NTRK1* juxtaposes exons 1-12 of *TRIM33* (ENST00000358465) to exons 12-17 of *NTRK1* (ENST00000524377). The fusion protein is predicted to include 1-732 AA of *TRIM33* and 452-796 AA of *NTRK1*. The whole tyrosine kinase domain encoded by *NTRK1* is retained in fusion.

In the sample PTC131, apart from the novel *TRIM33-NTRK1* fusion, we detected 4 other novel fusion transcripts of unknown significance: *ZSWIM5-TP53BP2*, *TAF4B-WDR1*, *ABI2-MTA3*, and *ARID1B-PSMA1* (Supporting Information Figures S2-S5). All 4 fusions apart from *ABI2-MTA3* are in-frame. *ABI2-MTA3* is out-of-frame and a premature stop codon occurs in 10th codon after the breakpoint.

We also found a novel in-frame isoform of the known oncogenic fusion *CCDC6-RET* in PTC106 sample (Supporting Information Figure S6). In the novel isoform, exons 1-8 of *CCDC6* (ENST00000263102) are fused to exons 12-20 of *RET* (ENST00000355710), in contrary to the most common *CCDC6-RET* rearrangement encompassing over 98% of cases, in which exon 1 of *CCDC6* is fused to exons 12-20 of the *RET* gene

(Supporting Information Figure S6).<sup>18</sup> The whole protein kinase domain encoded by *RET* is retained in the novel fusion isoform.

### 3.4 | Known fusion transcripts

Using RNA-Seq, *NCOA4-RET* (*RET/PTC1*) and *CCDC6-RET* (*RET/PTC3*) were found, as expected, in positive control samples. In the remaining samples, we also detected in-frame fusion transcripts already reported in the literature: two isoforms of *TFG-NTRK1*, *ETV6-NTRK3* (in 3 samples), *MKRN1-BRAF*, and *EML4-ALK* (Supporting Information Figures S7-S11). In all of them, 3' partner encodes tyrosine kinase domain, and the whole domain is retained in the predicted fusion protein.

In both the *TFG-NTRK1* isoforms that we detected, a fusion between exon 6 of *TFG* (ENST00000418917 or ENST00000240851) and exon 10 of *NTRK1* (ENST00000524377) was present. The two isoforms differed in the length of exon 6 of the *TFG* gene, which is 129 bp in *TFG* variant ENST00000418917 and 141 bp in *TFG* variant ENST00000240851 (Supporting Information Figures S7, S8). In *ETV6-NTRK3*, the fusion between exon 4 of *ETV6* (ENST00000396373) and exon 14 of *NTRK3* (ENST00000394480) was present (Supporting Information Figure S9). We detected *ETV6-NTRK3* in 3 samples, and it was the most prevalent alteration in our group. Two of three samples harboring *ETV6-NTRK3* were follicular variant of PTC. In *MKRN1-BRAF*, the fusion between exon 4 of *MKRN1* (ENST00000255977) and exon 11 of *BRAF* (ENST00000288602) was present (Supporting Information Figure S10). In *EML4-ALK*, the fusion between exon 13 of *EML4* (ENST00000318522)

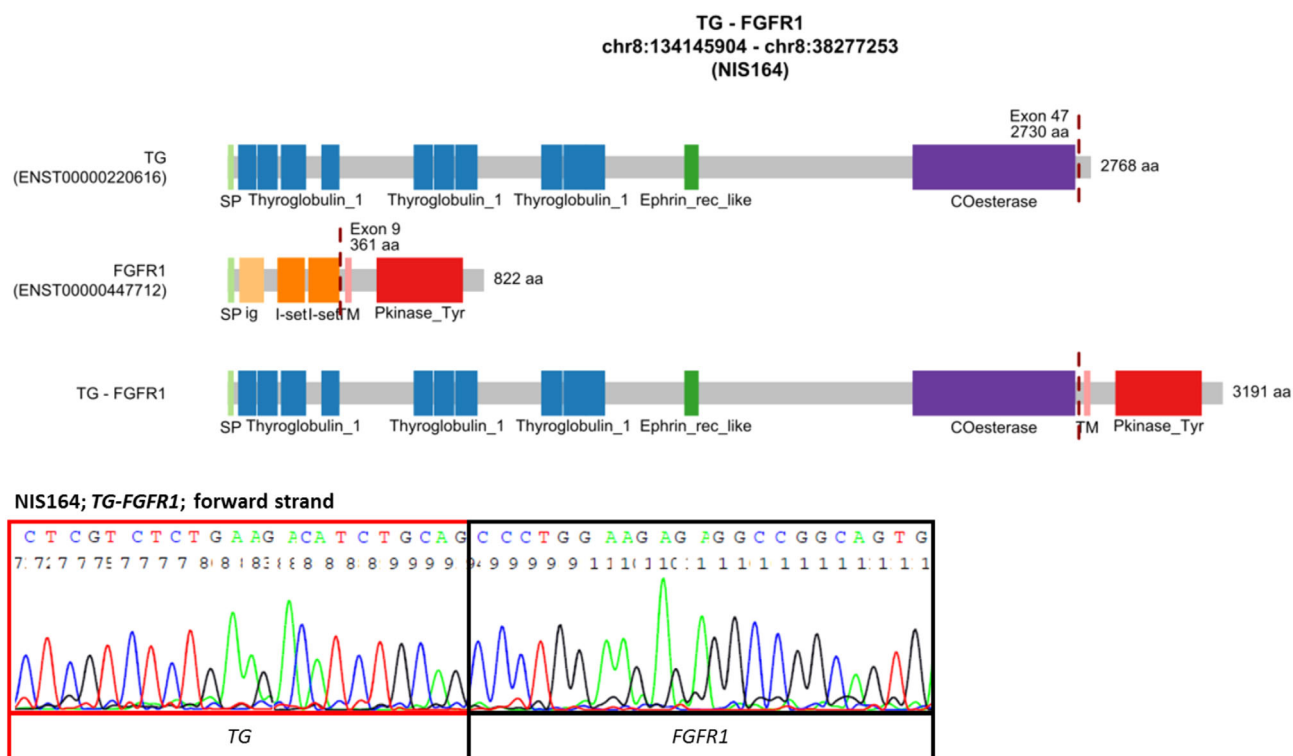


**FIGURE 1** The novel *TG-FGFR1* fusion transcript detected in PTC. The upper image shows the schematic diagram of the predicted fusion protein. The lower image shows the confirmation of the fusion transcript by direct Sanger sequencing. Abbreviations: COesterase, Carboxylesterase family; Ephrin\_rec\_like, Putative ephrin-receptor like; ig, Immunoglobulin domain; I-set, Immunoglobulin I-set domain; Pkinase\_Tyr, Protein tyrosine kinase; SP, signal peptide; Thyroglobulin\_1, Thyroglobulin type-1 repeat; TM, transmembrane region [Color figure can be viewed at [wileyonlinelibrary.com](http://wileyonlinelibrary.com)]



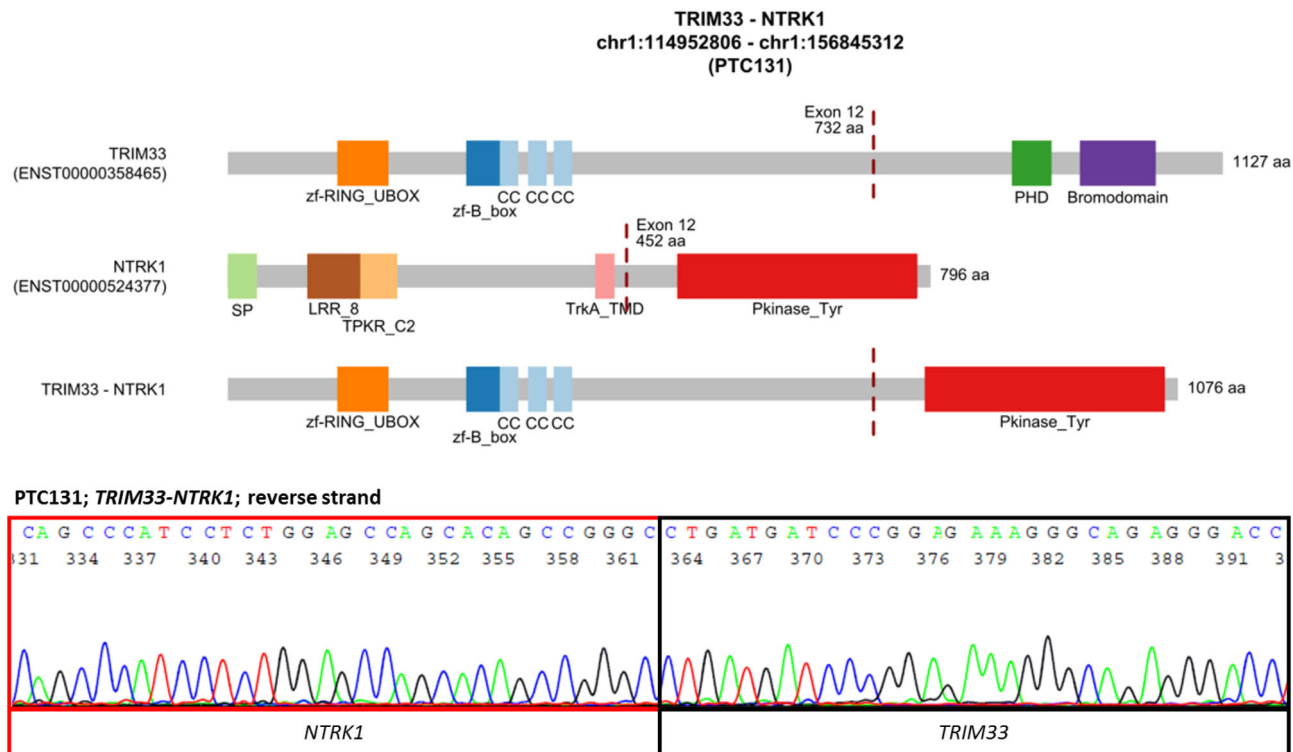


**FIGURE 2** The novel *TRIM33-NTRK1* fusion transcript detected in PTC. The upper image shows the schematic diagram of the predicted fusion protein. The lower image shows the confirmation of the fusion transcript by direct Sanger sequencing. Abbreviations: Bromodomain, Bromodomain; CC, coiled-coil region; LRR\_8, Leucine rich repeat; PHD, PHD-finger; Pkinase\_Tyr, Protein tyrosine kinase; SP, signal peptide; TPKR\_C2, Tyrosine-protein kinase receptor C2 Ig-like domain; TrkA\_TMD, Tyrosine kinase receptor A trans-membrane domain; zf-B\_box, B-box zinc finger; zf-RING\_UBOX, RING-type zinc-finger [Color figure can be viewed at [wileyonlinelibrary.com](http://wileyonlinelibrary.com)]

and exon 20 of *ALK* (ENST0000389048) was present (Supporting Information Figure S11).

## 4 | DISCUSSION

In this study, RNA-Seq was used to determine the presence of transcript fusions in PTCs. Fourteen PTC samples were examined, negative for the most common point mutations of the *BRAF* and *RAS* genes, and *PAX8-PPARG* rearrangements, with only 2 harboring *RET/PTC1* and *RET/PTC3* transcript fusions, treated as the positive controls. Among the analyzed samples novel fusion transcripts were found in two samples: *TG-FGFR1* and *TRIM33-NTRK1*, 7 demonstrated known fusion transcripts (*ETV6-NTRK3* in 3 samples, *TFG-NTRK1*, *EML4-ALK*, *MKRN1-BRAF*, and novel isoform of *CCDC6-RET*) and in 3 PTCs no fusion transcripts were detected. The tumor with *TRIM33-NTRK1* also carried 4 other transcript fusions of unknown significance: *ARID1B-PSMA1*, *TAF4B-WDR1*, *ABI2-MTA3*, and *ZSWIM5-TP53BP2*.

*TG-FGFR1* is a novel potentially oncogenic fusion transcript. TG is a glycoprotein homodimer produced predominantly by the thyroid gland. Only 1 case of TG fusion has been described so far in the literature: *TG-THADA*.<sup>1</sup> FGFR1, in turn, is a member of the FGFR family, which activation by mutations, amplification, or translocations plays roles in cancer initiation and development.<sup>19</sup> A number of *FGFR1*, *FGFR2*, and *FGFR3* rearrangements was identified in different cancers, including bladder cancer, breast cancer, head and neck cancer, lung squamous cell carcinoma, and thyroid cancer.<sup>20-22</sup> The *TG-FGFR1* fusion transcript found

in our PTC sample encodes a tyrosine kinase domain, which, when activated by TG, transmits the activation signal to the downstream effectors. It suggests that the *TG-FGFR1* may be responsible for cancer initiation and progression. The expression level of *TG-FGFR1* is driven by the promoter of *TG*, a gene with high expression in the thyroid, which may result in an aberrant overexpression of *TG-FGFR1*. One of the mechanisms that switches on the kinase domain in the fusion proteins is the dimerization by one of the domains present in the partner protein.<sup>23</sup> It has been shown that the cholinesterase-like domain located in C-terminal part of TG is responsible for dimerization.<sup>24</sup> This domain is preserved in the *TG-FGFR1* fusion protein and it may cause the FGFR1 domains to dimerize, resulting in activation of FGFR1 tyrosine kinase in the absence of ligands. The same sample harbored in addition a reciprocal fusion *FGFR1-TG*.

A second novel fusion detected in our PTC samples was the *TRIM33-NTRK1* rearrangement. *TRIM33* encodes a tripartite motif containing 33, a transcriptional corepressor, also known as *RFG7*. This gene has been demonstrated to create a fusion with the *RET* gene (*TRIM33-RET*) in radiation-induced thyroid carcinomas.<sup>25</sup> Similarly, *NTRK1* is also a known fusion partner gene in PTCs. *NTRK1* rearrangements occur in up to 13% of PTCs (12% in the Polish population).<sup>1,26-29</sup> The *TRIM33-NTRK1* fusion leads to activation of *NTRK1* tyrosine kinase domain, which in turn activates downstream effectors. The mechanism of tyrosine kinase activation in *TRIM33-NTRK1* may be similar to that in the *TRIM33-RET* fusion protein. *TRIM33* encodes a coiled-coil domain that allows ligand-independent dimerization of the chimeric protein and activation of

the truncated RET receptor in TRIM33-RET.<sup>30</sup> The TRIM33-NTRK1 fusion, similarly to *TG-FGFR1* rearrangement, may be a potential oncogene in PTC development. However, only in vitro functional studies can assess the role of the novel fusion proteins TG-FGFR1 and TRIM33-NTRK1 in PTC pathogenesis.

An additional 4 rearrangements (*ZSWIM5-TP53BP2*, *TAF4B-WDR1*, *ABI2-MTA3*, and *ARID1B-PSMA1*) were found in the PTC sample harboring the *TRIM33-NTRK1* rearrangement. These additional aberrations have not been described in any other cancer, and only *ABI2* and *ARID1B* have been involved in fusion genes. It is hence difficult to define the role of these fusions in tumorigenesis. It is possible that these fusions are a consequence of genomic instability and are secondary phenomena.

*ABI2* is a *KMT2A* translocation partner in acute myeloid leukemia.<sup>31</sup> *ABI2*, being a functional homologue of *ABI1*, is known as an *ABL1* regulator and is considered a tumor suppressor due to its inhibitory function in *ABL1* signaling. The *MTA3* gene is a member of the metastasis-associated protein family, identified as key regulators of the epithelial-mesenchymal transition process and E-cadherin expression.<sup>32</sup> *MTA3* has been described to be under-expressed in some malignancies, including breast cancer, ovarian cancer, gastroesophageal junction adenocarcinoma or endometrial cancer, and even as a suppressor of metastases in these tumors.<sup>33–35</sup> Shan et al<sup>36</sup> described decreased *MTA3* expression in glioma and its association with prognosis, which suggests that *MTA3* is a suppressor gene in this malignancy. Interestingly, the *ABI2-MTA3* fusion, found in our set of PTC samples, is out-of-frame and a premature stop codon occurs in 10th codon after the breakpoint, which may lead to silencing of *MTA3* expression. As regards the remaining 3 additional alterations, *ZSWIM5-TP53BP2*, *TAF4B-WDR1*, and *ARID1B-PSMA1*, they all represent in-frame fusions.

Fusion gene partners of the *TAF4B-WDR1* are the TATA-box binding protein associated factor 4b (*TAF4B*), involved in initiation of transcription of genes by RNA polymerase II, and WD repeat domain 1 (*WDR1*) involved in protein-protein interactions due to WD domains. *WDR1* plays a crucial role in cytokinesis and cell migration and may be important in the ability of cancer cells to proliferate and invade surrounding tissues.<sup>37,38</sup> Overexpression of *WDR1* was reported in different cancers, including breast cancer, ovarian carcinoma, and thyroid neoplasia.<sup>39–41</sup>

The fusion transcript *ZSWIM5-TP53BP2* is made of zinc finger SWIM-type containing 5 gene (*ZSWIM5*) and tumor protein TP53 binding protein 2 (*TP53BP2*, also known as *ASPP2*). *TP53BP2* is a member of the ASPP (apoptosis-stimulating protein of p53) family of TP53 interacting proteins, involved in apoptosis and cell growth regulation. It has been demonstrated that *TP53BP2* plays a role as a tumor suppressor<sup>42</sup> via interactions between Ank/SH3 domains, present in *TP53BP2*, and numerous partner proteins like TP53, NFKB1, and BCL2.<sup>43</sup> The fusion transcript, detected by us, retained the SH3 domain; however, it does not have ankyrin (Ank) repeats. Lack of these domains may inhibit *TP53BP2* tumor suppressor functions.

The last fusion, accompanying the *TRIM33-NTRK1* rearrangement, is the *ARID1B-PSMA1* fusion. *ARID1B* (AT-rich interaction domain 1B) encodes a protein that is a component of the SWI/SNF chromatin remodeling complex, which may play a role in cell-cycle activation. Tumor suppressor activity of *ARID1B* has been demonstrated in vitro in pancreatic cancer cells.<sup>44</sup> Moreover, deletions and mutations of this

gene have been reported in hepatocellular carcinoma, childhood neuroblastoma, PTC, and other types of cancer.<sup>45</sup> *ARID1B* has also been identified as an additional *ZNF384* fusion partner in pediatric acute lymphoblastic leukemia.<sup>46</sup> *PSMA1* (proteasome subunit alpha 1), in turn, was shown to be up-regulated in a number of cancers.<sup>47</sup>

We also detected novel in-frame isoform of the known oncogenic fusion *CCDC6-RET*, which similarly to other *RET* rearrangements, also retained the *RET* tyrosine kinase domain leading to *RET* activation.

In our group of samples, we also found 4 oncogenic fusions already reported in the literature: *TFG-NTRK1*, *ETV6-NTRK3*, *MKRN1-BRAF*, and *EML4-ALK*. *TFG-NTRK1* was previously reported in only a few PTC cases.<sup>27,48,49</sup> However, it was not reported in other cancers.<sup>18,50</sup> The longer of two isoforms detected in our study, TFG (exon 6 of ENST00000240851)–NTRK1 (exon 10 of ENST00000524377), has been already reported in PTC.<sup>1,51</sup> *ETV6-NTRK3* was the most prevalent alteration in PTC set analyzed by us, as it was found in 3 samples. According to the literature, the *ETV6-NTRK3* occurs in 2%–14.5% of PTC patients.<sup>8</sup> It also occurs in cancers of the salivary gland, kidney, and other tissues.<sup>18,50</sup> Two of the three samples harboring *ETV6-NTRK3* were follicular variants of PTCs. This is in agreement with recent findings that most post-Chernobyl PTCs in which *ETV6-NTRK3* was identified were classified as follicular variant of PTC.<sup>6,8</sup> The isoform detected in our study, which juxtaposes exon 4 of *ETV6* (ENST00000396373) and exon 14 of *NTRK3* (ENST00000394480), has been reported in PTC<sup>1,6,8,51</sup> and gastrointestinal stromal tumor.<sup>52</sup> *MKRN1-BRAF* has been reported in a few cases of PTC.<sup>1,7</sup> It was also described to be present in anaplastic thyroid cancer, pilocytic astrocytoma, head and neck neuroendocrine carcinoma, colon adenocarcinoma, and low-grade serous ovarian cancer.<sup>53–56</sup> The isoform detected in our study, which juxtaposes exon 4 of *MKRN1* (ENST00000255977) to exon 11 of *BRAF* (ENST00000288602), has been reported in pilocytic astrocytoma,<sup>54</sup> colon adenocarcinoma<sup>55</sup> and in low-grade serous ovarian cancer.<sup>56</sup> *EML4-ALK* was reported in PTC in a number of studies.<sup>1,9,57,58</sup> It also occurs in about 7% cases of non-small-cell lung cancer and in other cancers.<sup>50,59</sup> The isoform detected in our study, which juxtaposes exon 13 of *EML4* (ENST00000318522) and exon 20 of *ALK* (ENST00000389048) was reported in lung carcinoma<sup>59</sup> and papillary thyroid carcinoma.<sup>9,57</sup>

Although the number of analyzed PTC cases is small, they were carefully selected, and only young PTC patients without known somatic mutations of the *BRAF* and *RAS* genes, *PAX8-PPARG*, *RET/PTC1*, and *RET/PTC3* rearrangements were taken into consideration. We found new fusion transcripts with a potential oncogenic role and a number of known rearrangements. Our study shows that although large analyses like TCGA study gave us a lot of new data about PTC biology, still some information is missing, and further analyses are needed. There is no doubt that better understanding of molecular PTC background will open new diagnostic and therapeutic possibilities.

## ORCID

Aleksandra Pfeifer  <https://orcid.org/0000-0002-0189-9711>

Joanna Polańska  <https://orcid.org/0000-0001-8004-9864>

## REFERENCES

- Cancer Genome Atlas Research Network. Integrated genomic characterization of papillary thyroid carcinoma. *Cell*. 2014;159:676-690.
- Su X, Li Z, He C, Chen W, Fu X, Yang A. Radiation exposure, young age, and female gender are associated with high prevalence of RET/PTC1 and RET/PTC3 in papillary thyroid cancer: a meta-analysis. *Oncotarget*. 2016;7:16716-16730.
- Cantara S, Capezzone M, Marchisotta S, et al. Impact of proto-oncogene mutation detection in cytological specimens from thyroid nodules improves the diagnostic accuracy of cytology. *J Clin Endocrinol Metab*. 2010;95:1365-1369.
- Nikiforov YE, Carty SE, Chiosea SI, et al. Impact of the multi-gene ThyroSeq next-generation sequencing assay on cancer diagnosis in thyroid nodules with atypia of undetermined significance/follicular lesion of undetermined significance cytology. *Thyroid*. 2015;25:1217-1223.
- Guerra A, Sapio MR, Marotta V, et al. Prevalence of RET/PTC rearrangement in benign and malignant thyroid nodules and its clinical application. *Endocr J*. 2011;58:31-38.
- Ricarte-Filho JC, Li S, Garcia-Rendueles MER, et al. Identification of kinase fusion oncogenes in post-Chernobyl radiation-induced thyroid cancers. *J Clin Invest*. 2013;123:4935-4944.
- Smallridge RC, Chindris A-M, Asmann YW, et al. RNA sequencing identifies multiple fusion transcripts, differentially expressed genes, and reduced expression of immune function genes in BRAF (V600E) mutant vs BRAF wild-type papillary thyroid carcinoma. *J Clin Endocrinol Metab*. 2014;99:E338-E347.
- Leeman-Neill RJ, Kelly LM, Liu P, et al. ETV6-NTRK3 is a common chromosomal rearrangement in radiation-associated thyroid cancer. *Cancer*. 2014;120:799-807.
- Kelly LM, Barila G, Liu P, et al. Identification of the transforming STRN-ALK fusion as a potential therapeutic target in the aggressive forms of thyroid cancer. *Proc Natl Acad Sci U S A*. 2014;111:4233-4238.
- Costa V, Esposito R, Ziviello C, et al. New somatic mutations and WNK1-B4GALNT3 gene fusion in papillary thyroid carcinoma. *Oncotarget*. 2015;6:11242-11251.
- Yoo SK, Lee S, Kim SJ, et al. Comprehensive analysis of the transcriptional and mutational landscape of follicular and papillary thyroid cancers. *PLoS Genet*. 2016;12:1-23.
- Andrews S. FastQC: A quality control tool for high throughput sequence data. <http://www.bioinformatics.babraham.ac.uk/projects/fastqc/>.
- Schmieder R, Edwards R. Quality control and preprocessing of metagenomic datasets. *Bioinformatics*. 2011;27:863-864.
- Kim D, Salzberg SL. TopHat-Fusion: an algorithm for discovery of novel fusion transcripts. *Genome Biol*. 2011;12:R72.
- Iyer MK, Chinnaiyan AM, Maher CA. ChimeraScan: a tool for identifying chimeric transcription in sequencing data. *Bioinformatics*. 2011;27:2903-2904.
- Asmann YW, Hossain A, Necela BM, et al. A novel bioinformatics pipeline for identification and characterization of fusion transcripts in breast cancer and normal cell lines. *Nucleic Acids Res*. 2011;39:e100.
- Babiceanu M, Qin F, Xie Z, et al. Recurrent chimeric fusion RNAs in non-cancer tissues and cells. *Nucleic Acids Res*. 2016;44:2859-2872.
- Forbes SA, Beare D, Boutselakis H, et al. COSMIC: somatic cancer genetics at high-resolution. *Nucleic Acids Res*. 2017;45:D777-D783.
- Brooks AN, Kilgour E, Smith PD. Molecular pathways: fibroblast growth factor signaling: a new therapeutic opportunity in cancer. *Clin Cancer Res*. 2012;18:1855-1862.
- Wu Y-M, Su F, Kalyana-Sundaram S, et al. Identification of targetable FGFR gene fusions in diverse cancers. *Cancer Discov*. 2013;3:636-647.
- Parker BC, Engels M, Annala M, Zhang W. Emergence of FGFR family gene fusions as therapeutic targets in a wide spectrum of solid tumours. *J Pathol*. 2014;232:4-15.
- Wang R, Wang L, Li Y, et al. FGFR1/3 tyrosine kinase fusions define a unique molecular subtype of non-small cell lung cancer. *Clin Cancer Res*. 2014;20:4107-4114.
- Medves S, Demoulin J-B. Tyrosine kinase gene fusions in cancer: translating mechanisms into targeted therapies. *J Cell Mol Med*. 2012;16:237-248.
- Lee J, Wang X, Di Jeso B, Arvan P. The cholinesterase-like domain, essential in thyroglobulin trafficking for thyroid hormone synthesis, is required for protein dimerization. *J Biol Chem*. 2009;284:12752-12761.
- Rabes HM. Gene rearrangements in radiation-induced thyroid carcinogenesis. *Med Pediatr Oncol*. 2001;36:574-582.
- Bongarzone I, Fugazzola L, Vigneri P, et al. Age-related activation of the tyrosine kinase receptor protooncogenes RET and NTRK1 in papillary thyroid carcinoma. *J Clin Endocrinol Metab*. 1996;81:2006-2009.
- Musholt TJ, Musholt PB, Khaladj N, Schulz D, Scheumann GFW, Klemmner J. Prognostic significance of RET and NTRK1 rearrangements in sporadic papillary thyroid carcinoma. *Surgery*. 2000;128:984-993.
- Rabes HM, Demidchik EP, Sidorow JD, et al. Pattern of radiation-induced RET and NTRK1 rearrangements in 191 post-Chernobyl papillary thyroid carcinomas: biological, phenotypic, and clinical implications. *Clin Res Cancer*. 2000;6:1093-1103.
- Brzezińska E, Karbownik M, Migdalska-Sek M, Pastuszak-Lewandoska D, Włoch J, Lewiński A. Molecular analysis of the RET and NTRK1 gene rearrangements in papillary thyroid carcinoma in the Polish population. *Mutat Res*. 2006;599:26-35.
- Nikiforov YE. RET/PTC rearrangement in thyroid tumors. *Endocr Pathol*. 2002;13:3-16.
- Coenen EA, Zwaan CM, Meyer C, et al. Abl-interactor 2 (ABI2): a novel MLL translocation partner in acute myeloid leukemia. *Leuk Res*. 2012;36:e113-e115.
- Toh Y, Nicolson GL. The role of the MTA family and their encoded proteins in human cancers: molecular functions and clinical implications. *Clin Exp Metastasis*. 2009;26:215-227.
- Fearon ER. Connecting estrogen receptor function, transcriptional repression, and E-cadherin expression in breast cancer. *Cancer Cell*. 2003;3:307-310.
- Dong H, Guo H, Xie L, et al. The metastasis-associated gene MTA3, a component of the Mi-2/NuRD transcriptional repression complex, predicts prognosis of gastroesophageal junction adenocarcinoma. *PLoS One*. 2013;8:e62986.
- Bruning A, Juckstock J, Blankenstein T, Makovitzky J, Kunze S, Mylonas I. The metastasis-associated gene MTA3 is downregulated in advanced endometrioid adenocarcinomas. *Histol Histopathol*. 2010;25:1447-1456.
- Shan S, Hui G, Hou F, et al. Expression of metastasis-associated protein 3 in human brain glioma related to tumor prognosis. *Neural Sci*. 2015;36:1799-1804.
- Kato A, Kurita S, Hayashi A, Kaji N, Ohashi K, Mizuno K. Critical roles of actin-interacting protein 1 in cytokinesis and chemotactic migration of mammalian cells. *Biochem J*. 2008;414:261-270.
- Hanahan D, Weinberg RA. Hallmarks of cancer: the next generation. *Cell*. 2011;144:646-674.
- Haslene-Hox H, Oveland E, Woie K, Salvesen HB, Wiig H, Tenstad O. Increased WD-repeat containing protein 1 in interstitial fluid from ovarian carcinomas shown by comparative proteomic analysis of malignant and healthy gynecological tissue. *Biochim Biophys Acta*. 2013;1834:2347-2359.
- Izawa S, Okamura T, Matsuzawa K, et al. Autoantibody against WD repeat domain 1 is a novel serological biomarker for screening of thyroid neoplasia. *Clin Endocrinol (Oxf)*. 2013;79:35-42.
- Kim D-H, Bae J, Lee JW, et al. Proteomic analysis of breast cancer tissue reveals upregulation of actin-remodeling proteins and its relevance to cancer invasiveness. *Proteomics Clin Appl*. 2009;3:30-40.
- Van Hook K, Wang Z, Chen D, et al. DeltaN-ASPP2, a novel isoform of the ASPP2 tumor suppressor, promotes cellular survival. *Biochem Biophys Res Commun*. 2017;482:1271-1277.
- Rotem S, Katz C, Benyamini H, et al. The structure and interactions of the proline-rich domain of ASPP2. *J Biol Chem*. 2008;283:18990-18999.
- Khursheed M, Kolla JN, Kotapalli V, et al. ARID1B, a member of the human SWI/SNF chromatin remodeling complex, exhibits tumour-suppressor activities in pancreatic cancer cell lines. *Br J Cancer*. 2013;108:2056-2062.



45. Vengoechea J, Carpenter L, Zarate YA. Papillary thyroid cancer in a patient with interstitial 6q25 deletion including ARID1B. *Am J Med Genet A*. 2014;164A:1857-1859. 164.
46. Shago M, Abla O, Hitzler J, Weitzman S, Abdelhaleem M. Frequency and outcome of pediatric acute lymphoblastic leukemia with ZNF384 gene rearrangements including a novel translocation resulting in an ARID1B/-ZNF384 gene fusion. *Pediatr Blood Cancer*. 2016;63:1915-1921.
47. Li Y, Huang J, Sun J, et al. The transcription levels and prognostic values of seven proteasome alpha subunits in human cancers. *Oncotarget*. 2017;8:4501-4519.
48. Greco A, Mariani C, Miranda C, et al. The DNA rearrangement that generates the TRK-T3 oncogene involves a novel gene on chromosome 3 whose product has a potential coiled-coil domain. *Mol Cell Biol*. 1995;15:6118-6127.
49. Mencinger M, Panagopoulos I, Andreasson P, Lassen C, Mitelman F, Aman P. Characterization and chromosomal mapping of the human TFG gene involved in thyroid carcinoma. *Genomics*. 1997;41:327-331.
50. Mitelman F, Johansson B, Mertens F. Mitelman database of chromosome aberrations and gene fusions in cancer. <http://cgap.nci.nih.gov/Chromosomes/Mitelman>. Published 2018.
51. Hu X, Wang Q, Tang M, et al. TumorFusions: an integrative resource for cancer-associated transcript fusions. *Nucleic Acids Res*. 2018;46:D1144-D1149.
52. Brenca M, Rossi S, Polano M, et al. Transcriptome sequencing identifies ETV6 - NTRK3 as a gene fusion involved in GIST. *J Pathol*. 2016;238:543-549.
53. Kasaian K, Wiseman SM, Walker BA, et al. The genomic and transcriptomic landscape of anaplastic thyroid cancer: implications for therapy. *BMC Cancer*. 2015;15:1-11.
54. Jones DTW, Hutter B, Jäger N, et al. Recurrent somatic alterations of FGFR1 and NTRK2 in pilocytic astrocytoma. *Nat Genet*. 2013;45:927-932.
55. Ross JS, Wang K, Chmielecki J, et al. The distribution of BRAF gene fusions in solid tumors and response to targeted therapy. *Int J Cancer*. 2016;138:881-890.
56. Grisham RN, Sylvester BE, Won H, et al. Extreme outlier analysis identifies occult mitogen-activated protein kinase pathway mutations in patients with low-grade serous ovarian cancer. *J Clin Oncol*. 2015;33:4099-4105.
57. Hamatani K, Mukai M, Takahashi K, Hayashi Y, Nakachi K, Kusunoki Y. Rearranged anaplastic lymphoma kinase (ALK) gene in adult-onset papillary thyroid cancer amongst atomic bomb survivors. *Thyroid*. 2012;22:1153-1159.
58. Demeure MJ, Aziz M, Rosenberg R, Gurley SD, Bussey KJ, Carpten JD. Whole-genome sequencing of an aggressive BRAF wild-type papillary thyroid cancer identified EML4-ALK translocation as a therapeutic target. *World J Surg*. 2014;38:1296-1305.
59. Soda M, Choi YL, Enomoto M, et al. Identification of the transforming EML4-ALK fusion gene in non-small-cell lung cancer. *Nature*. 2007;448:561-566.

## SUPPORTING INFORMATION

Additional supporting information may be found online in the Supporting Information section at the end of the article.

**How to cite this article:** Pfeifer A, Rusinek D, Žebracka-Gala J, et al. Novel *TG-FGFR1* and *TRIM33-NTRK1* transcript fusions in papillary thyroid carcinoma. *Genes Chromosomes Cancer*. 2019; 58:558-566. <https://doi.org/10.1002/gcc.22737>